

# Full densification of Molybdenum powders using Spark Plasma Sintering

B. Mouawad<sup>1</sup>, M. Soueidan<sup>1,2</sup>, D. Fabrègue<sup>3</sup>, C. Buttay<sup>1\*</sup>, V. Bley<sup>4</sup>, B. Allard<sup>1</sup> and H. Morel<sup>1</sup>

<sup>1</sup> Université de Lyon, INSA de Lyon, AMPERE-UMR 5005, Bât. L. de Vinci, 21, Av. J. Capelle, 69621 Villeurbanne Cedex – France.

<sup>2</sup> Lebanese Atomic Energy Commission, P.O. Box 11-8281, Riad El Solh 1107 2260 Beirut, Lebanon.

<sup>3</sup> Université de Lyon, INSA de Lyon, MATEIS-UMR 5510, Bât. B.PASCAL, 7 avenue J. Capelle, F-69621 Villeurbanne Cedex, France.

<sup>4</sup> Université de Toulouse, UPS, INPT, LAPLACE 118, route de Narbonne, 31062 Toulouse, France.

[bassem.mouawad@insa-lyon.fr](mailto:bassem.mouawad@insa-lyon.fr), [maher.soueidan@insa-lyon.fr](mailto:maher.soueidan@insa-lyon.fr), [damien.fabregue@insa-lyon.fr](mailto:damien.fabregue@insa-lyon.fr), [cyril.buttay@insa-lyon.fr](mailto:cyril.buttay@insa-lyon.fr), [vincent.bley@laplace.univ-tlse.fr](mailto:vincent.bley@laplace.univ-tlse.fr), [bruno.allard@insa-lyon.fr](mailto:bruno.allard@insa-lyon.fr)

## Abstract:

Pure molybdenum powder was sintered using Spark Plasma Sintering under various temperatures, and holding times, under a pressure of 77 MPa and a heating rate at 700°C/min. After sintering, a carbide layer was observed at the surface. The carbide layer thickness, the relative density of the sample as well as the microhardness and the grain size of Mo were measured. The carbide thickness depends on time and temperature and it was found that the carbide layer grows in a parabolic manner, with the activation energy of carbon diffusion in Mo being equal to 34 Kcal/mol. The densification of Mo is controlled mainly by the sintering temperature and the holding time. The molybdenum powder was successfully consolidated by SPS in short times. A relative density of 100% is achieved at a sintering temperature of 1850°C and a holding time of 30 minutes. It was shown that the hardness decreases slightly with temperature and time. It should be related to the increase in grain size with the sintering temperature and time.

Corresponding author: Maher SOUEIDAN

E-mail: [maher.soueidan@insa-lyon.fr](mailto:maher.soueidan@insa-lyon.fr)

Postal Address: Université de Lyon, INSA de Lyon, AMPERE-UMR 5005, Bât. L. de Vinci, 21, Av. J. Capelle, 69621 Villeurbanne Cedex – France

Tel: +33 (4) 72 43 79 11  
Fax : +33 (4) 72 43 85 30

**Keyword:** Molybdenum, Spark Plasma Sintering, densification, microstructure.

## I. Introduction

Molybdenum has a body-centered cubic structure with a melting point of 2610°C and a density of 10.22 g/cm<sup>3</sup> and presents a great potential to become an important refractory metal. The refractory properties of molybdenum reflect the high strength of its inter-atomic bonding [1]. This material has been used for high temperature applications in a variety of industries. In addition, the relatively low thermal neutron cross-section of Mo makes it suitable for nuclear applications. The unique combination of physical, chemical and mechanical properties of Mo makes it an ideal material for a variety of engineering applications where high temperature resistance, and ductility are key issues [1–5].

Molybdenum has been used in many electronic applications from the earlier days of the technology. This metal combines both satisfying thermal conductivity (142W/m.K at 20°C) and a coefficient of thermal Expansion (CTE) which offers a good match with that of silicon (4.8 and 2.6 ppm/°C at 25°C respectively). Thanks to that large area silicon devices (up to 10 cm in diameter) can be directly bonded onto a molybdenum disk to improve their mechanical strength in high power, press-pack packages [6]. Such components have been manufactured for several decades, using molybdenum disks directly stamped from fully dense wrought sheet. In this way, the deleterious effects of residual porosity on the thermal conductivity are eliminated.

Generally, powder metallurgy (P/M) has been used for the production of bulk Mo components [3–5]. High sintering temperatures, in the range of 1800 - 2000°C, with long sintering times, are required for densification above 90% of the theoretical density for refractory metals. Because of the difficulty in achieving full-densification of Mo, much research focused on the enhancement of the sinterability. In this regard, one of the suggested processes for enhancing sinterability is the activated sintering process in which a metal such as Ni, Pt, Pd or Co is added to Mo [7–13]. However, these elements can degrade the electrical and thermal properties of the Mo. To achieve nearly full density in short processing time intervals, while concurrently minimizing grain growth-related degradation of mechanical

properties, a few non-conventional techniques have been reported. Explosive consolidation [14-17], ceracon rapid omni-directional ROC [18-20], plasma-activated sintering PAS [21,22], microwave sintering [23,24], are a few of the rapid consolidation techniques reported in the literature. First studies on short-time sintering of molybdenum powders by Plasma Pressure Compaction (P<sup>2</sup>C) are reported in [25,26]. Micro-sized powders (average size 47 μm) were consolidated at 1650°C, 48 MPa, for 1-2 min, up to a relative density of 97%. Nano-sized powders (average size 0.1 μm) were sintered at lower temperature (1400°C), 48 MPa, for 3 min, with a relative density of 97%. Nano- and micro-sized consolidated samples showed a microhardness varying from 2.18 GPa (222 Hv) to 2.16 GPa (220 Hv) respectively.

Spark plasma sintering (SPS) is a technique developed in the 50's that enables ceramic or metal powder to be fully densified at relatively low temperature and in very short time [27,28]. It is similar to conventional hot-pressing, but the heating is obtained by applying an intense pulsed current through electrodes located on top and bottom of a sintering die. This current was first thought to generate spark discharge at the interface between particles, activating and purifying the particles surface [29] but now, the absence of plasma seems to be generally admitted [30]. Anyway the presence of current seems to lead heat and mass transfer to be completed in extremely short time. Further advantages are sintering of powder without any additives, no need for cold compaction and lower sensitivity to the initial powders characteristics. SPS is therefore an economical alternative to conventional sintering. Recently, Ohser-Wiedemann et al. have achieved a relative density of 95% of a sintered bulk of micro-powder molybdenum using SPS at 1600°C, an external pressure of 67 MPa and a holding time at maximum temperature of 3 min. Moreover, the hardness of all investigated samples are in the same range, independent from the sintering conditions. The average hardness is 2.05 GPa (209 Hv) [31].

In this research paper, we investigate the consolidation of Molybdenum powders by Spark Plasma Sintering. We study the influence of SPS processing conditions on the density, hardness and grain size of bulk molybdenum specimens. In certain conditions the final density obtained was 100%.

## **II. Experimental procedures**

Commercial Molybdenum powder (Goodfellow, Cambridge, UK, 99.99+% purity) with a particle size ranging from 55μm to 355 μm was consolidated by the SPS technique. The as-

received powder was found to have an average grain size equal to 16  $\mu\text{m}$  (see figure 1). In this technique, molybdenum powders were poured directly, with no special treatment into a cylindrical graphite die and without any additive or binder. The experiments were carried out using the SPS equipment (FCT HPD 25) available at the MATEIS laboratory.

In each experiment, the molybdenum powders are introduced in a carbon die of 20 mm inner diameter. Samples 20 mm in diameter and 2 mm high were sintered in vacuum ( $10^{-2}$  Torr), with temperatures ranging from 1200 to 1950°C. The uniaxial pressure was fixed at 77 MPa during the consolidation and maintained during the cooling down to room temperature. This pressure corresponds to the maximum pressure that the graphite die can sustain. The temperature was measured with an optical pyrometer focused on the surface of the graphite die (see figure 2) and automatically regulated from 600 °C to the final sintering temperature. The temperature of 600 °C was reached via a preset heating program as the pyrometer could not sense low temperature (below 600 °C). The heating rate was fixed to 700 °C/min and the sintering time was varied from 5 to 30 minutes. It is important to note that carbon foils were placed under and below the powder to assure an easy dismantling of the sintered samples.

To study the microstructure, the samples were prepared for examination in optical microscopy to identify: 1) the grain size and morphology, and 2) the presence and distribution of processing related defects. The defect features include: a) irregular surface cracks, b) string-like and angular features, and c) microscopic pores and voids. The surfaces and cross sections (sections parallel to the sintering pressure) of the sintered samples were ground and polished. An initial wet grind and coarse polish on progressively finer grades of Buehler's Ultra Plan, Ultra Pad and Texmet polishing cloths. Finish polishing was achieved using 1  $\mu\text{m}$  diamond paste. The samples were then cleaned to remove the lubricant. The cleaning process found to be successful consisted of (i) ultrasonic cleaning in acetone to remove the lubricant, (ii) ultrasonic cleaning in trichloroethylene, (iii) ultrasonic cleaning in microelectronic grade ethanol, (iv) followed by rinsing in DI water and blow drying with nitrogen gas. The as-polished samples were wet chemically etched in  $\text{H}_2\text{SO}_4:\text{HNO}_3:\text{H}_2\text{O}$  (1:1:1) for about 1 minute.

The polished and etched samples were also examined by scanning electron microscope (SEM), with the objective of determining the morphology and distribution of sintering defects porosity. The SEM study was performed on a Philips XL20.

Precise density measurements of the consolidated bulk molybdenum samples were made using the Archimedes' principle according to ASTM Standard B328-94. The relative

density was calculated based on the theoretical density of Mo ( $10.22 \text{ g/cm}^3$ ) listed in [1].

The microhardness and hardness measurements have been realized on a Vickers machine Wolpert (V-testor VDT 11) using a 0.3 kg charge and a Shimadzu HSV 20 using a 5 Kg charge. The hardness value given for each sample is the average of at least 10 measurements taken randomly.

The grain size was measured using an optical microscope coupled to the image analysis software Grani. The method used to calculate the grain size is the intercept one (ASTM 112). For elementary analyses, Secondary Ion Mass Spectroscopy (SIMS) measurements were done using a Cameca IMS 4f spectrometer with  $\text{O}^{2+}$  primary ion source. The impact energy was 15 keV.

For structural analysis, the samples were characterized by X-ray diffraction (XRD: X'Pert Pro MPD from Panalytical, equipped with an X'Celerator detector monochromator, CuKalpha radiation, Almelo, The Netherlands).

### **III. Experimental results and discussion**

#### *III.1. Molybdenum carbide formation*

In order to check the SPS consolidated samples, the cross-sectional microstructure was imaged using an optical microscope with bright field illumination for low magnifications and a SEM at higher magnifications. Representative optical micrograph and scanning electron micrograph are shown in fig. 3.a and 3.b. This microstructure has been obtained for sintering at  $1850^\circ\text{C}$  for 5 min, with a pressure of 77 MPa. Two different zones can be observed in both images. The first one is localized near to the surface (M1) and the second one is in the center of the sample (M2). Moreover, the interface between both microstructures is clearly visible. This interface is not straight and shows large waves. The average thickness of the first zone M1 is equal to  $115 \mu\text{m}$ . The cross sectional hardness measurements made at different locations from the surface to the inner of the sample exhibit a large hardness gradient. The average hardness value was found to be 1400 HV0.3 and 173 HV0.3 in the M1 and M2 regions respectively. That means that the nature of the materials is not the same between the two different zones. The average hardness value of M2 at 173 HV0.3 should correspond to molybdenum; this will be discussed in the next section. In contrast, the hardness value of M1 at 1400 HV0.3 corresponds to a material formed during sintering, whose identification is

discussed below. It is worth noticing that no additive was added to the molybdenum.

Secondary Ion Mass Spectroscopy (SIMS) was performed on the M1 layer for elementary analysis to deduce the elementary composition of the layer. The SIMS spectrum in figure 4 clearly shows that the layer contains only two elements (Mo and C). This means that the M1 layer is composed by Mo and C, which corresponds to molybdenum carbide.

Molybdenum carbide exists in two stable crystalline forms:  $\alpha$ -Mo<sub>2</sub>C and  $\beta$ -Mo<sub>2</sub>C [32,33]. The structure of  $\beta$ -Mo<sub>2</sub>C is hexagonal close packed (hcp) and the structure of  $\alpha$ -Mo<sub>2</sub>C is orthorhombic. The XRD patterns of the samples surface were recorded at room temperature in the  $2\theta$  range 30-80° ( $2\theta$ ) in step of 0.1° in Fig. 5. In all cases, the diffraction patterns recorded were characteristic of the  $\beta$ -Mo<sub>2</sub>C [34]. The  $\beta$ -Mo<sub>2</sub>C peaks correspond to ( $2\theta = 34.4, 38.0, 39.4, 52.1, 61.5, 69.6$  and  $74.6$  for  $\beta$ -Mo<sub>2</sub>C orientations along the crystallographic directions [100], [002], [101], [102], [110], [103] and [200], respectively. One other peak was detected and can be attributed to molybdenum.

Table 1 gathers all the results from the sintering experiments in terms of carbide thickness, densities, hardness and grain size. From table 1, one can see that the molybdenum carbide is obtained during sintering at high temperature (>1500°C). This means that the carbide layer was not observed at lower temperature, but it could be due to the removing of the thin carbide layer at the same time as the carbon foil. In order to clarify the formation of molybdenum carbide, it is important to identify the source of carbon involved in the formation of this molybdenum carbide. The only possible C source in contact with the Mo powders is the graphite die and the carbon foil because they are the only elements in contact with Mo powders.

The growth of the molybdenum carbide layer formed at 1850°C and at 77 MPa is shown in Fig. 6. In this figure, the square of the thickness is plotted against time. The thickness values plotted are the average values of the Mo<sub>2</sub>C formed over more than 10 measurements. The results presented in this figure show, as expected, a linear increase in product thickness with time. In that case, only the sintering time is taken into account since the heating rate as well as the cooling rate is high. This assumption could involve some errors for shorter times.

Fig. 7 presents the evolution of the growth rate as a function of the inverse of the temperature. One can see that the growth rate increases when the temperature increases. From

the Arrhenius plot of Fig. 7 the apparent activation energy ( $E_A$ ) of the growth process was calculated.  $E_A$  was estimated to be equal to 34 Kcal/mol (142.3 KJ/mol), which is close to the values found in the literature [31, 35, 36].

### *III.2. Molybdenum consolidation*

#### *III.2.1. Density*

To measure the actual density of our Mo samples, the  $\text{Mo}_2\text{C}$  layers were removed from both sides by polishing. The calculated relative densities with and without carbide layers are listed in table 1. We can see that the relative density without carbide is higher than the one with carbide at a given sintering parameter. This can be explained by the difference in density between  $\text{Mo}_2\text{C}$  ( $8.9 \text{ g/cm}^3$ ) and Mo ( $10,22 \text{ g/cm}^3$ ).

Fig 8 (a and b) shows the relative densities of the sintered samples without the carbide layer as a function of temperature and holding times respectively. It was shown that the relative density increases with sintering temperature for a given time (5 min) and pressure (77 MPa) (see fig 8a). In this case, the maximum relative density of 99.5% can be reached at a sintering temperature of  $1950^\circ\text{C}$ . Moreover, our results are in good agreement with previous results obtained by  $\text{P}^2\text{C}$  [25,26] and SPS [31], where a relative density of 98% was measured at  $1650^\circ\text{C}$  for  $\text{P}^2\text{C}$  and 95% at  $1600^\circ\text{C}$  for SPS. Fig. 8b shows the relationship between the relative density and the holding time at  $1850^\circ\text{C}$  and 77 MPa. This demonstrates that when the holding time is increased from 5 to 30 minutes, the relative density increases from 98.6 % to 100%. To our knowledge, a relative density of 100% for molybdenum has never been reported yet using a sintering technique.

#### *III.2.2. Hardness*

Vickers hardness measurements made at different locations on the surface of each samples are summarized in table 1. The samples were polished to a mirror finish before the hardness measurement. The measured hardness was observed to be near-uniform throughout each sintered sample, indicating uniform densification. Polishing of the sample surface reduces the spread in measured hardness values. Fig. 8 (a and b) shows the variation of the hardness as a function of temperature and holding time respectively. At  $1200$  and  $1350^\circ\text{C}$ , the samples were not totally densified, so the hardness measurement are not representative. The hardness decreases very slightly when increasing the sintering temperature (it varies from 160 at  $1450^\circ\text{C}$  to 149 Hv5 at  $1950^\circ\text{C}$ , see fig. 8a) as well as when increasing holding time. This

decrease in hardness could be explained by the increase of grain size with temperature (Hall and Petch relationship). This will be explored in the next section. In both cases, the variation of hardness is very slight and could be simply due to experimental scattering.

The hardness values obtained in this study could be compared to the ones already published. However, the literature concerning the hardness exhibits high variations according to the initial state of the powders and to the process parameters used for their sintering. For example, Tuminen and Dahl [37] reported microhardness values of about 270 Hv 10 for unsintered Mo powder extrusions, and 250 Hv 10 for conventionally sintered Mo bars. These high values are easily understandable since the powder come from extrusion and thus must be highly deformed leading to a high hardness value. Kim et al. [38] obtained hardness values equal to 218 Hv 0.1 for nanopowder and 191 Hv0.1 for commercial powder, which is in agreement with our results taking into account the measurement errors. At last, Srivatsan et al. [26,39] reported hardness values of about 236 Hv10 by Plasma Pressure Compact with consolidation at a temperature of 1650°C for Mo powder (grain size of about 47  $\mu\text{m}$ ). Finally, using SPS techniques, R. Ohser-Wiedemann [31] reported an average hardness value of about 209 Hv 0.1, independently on sintering condition, which is consistent with the values obtained in this study.

### *III.2.3. Grain size*

The cross-sectional microstructure of molybdenum sintered at 1850 °C for 5 min, and with a pressure of 77 MPa is shown in Fig. 9a after wet chemical etching in  $\text{H}_2\text{SO}_4:\text{HNO}_3:\text{H}_2\text{O}$  (1:1:3). No pores were observed between the grains. It was found that the average grain size (82  $\mu\text{m}$ ) is larger than the initial average grain size (16 $\mu\text{m}$ ). Fig. 9b shows the grain size distribution and we can also see that the grains grow discontinuously. From fig. 9a and b could suggest that secondary recrystallization occurs during sintering. Fig. 9 (c and d) shows the variation of average grain size as a function of temperature and time respectively. The sintering temperature has a significant effect on grain size. When the sintering temperature is under 1450°C, the grain growth is slow and limited, the average grain size remains equal to the initial grain size (16  $\mu\text{m}$ ). When the sintering temperature rises from 1450 to 1950°C, the grains grow significantly, with an average grain size ranging from 33  $\mu\text{m}$  to 108  $\mu\text{m}$  respectively (shown in fig. 9c). Comparing to those in the literature, the same phenomena was obtained with the ref [31]: the grain size start increasing at high temperature (higher than 1400). This result was obtained by SPS. In contrast, when using a conventional technique

such as isothermal sintering the grain growth starts at temperature lower than 1100°C [38]. This big difference may be due to the fast heating ramp of the SPS. Note that the comparison of the average grain values is very difficult because the as-received Mo powder and grain size are not the same.

The relationship between the grain size and the holding time is presented in fig. 9d. In this series of experiments, the temperature was set to 1850°C, the pressure to 77 MPa and the sintering time ranged from 5 to 30 minutes. This demonstrates that when the holding time is increased from 5 to 30 min, the grain size increases from 82 to 102  $\mu\text{m}$ . This difference in grain size growth can be explained by the fact that grain grows with an exponential function of the temperature but follows a logarithmic law according to the time.

Considering the maximal sintering temperature is 1950°C, It can be concluded that the main temperature range to affect the grain growth is 1450-1950°C. Below 1450°C, the sample exhibits a low density (less than 95%). Thus the heat generated by Joule Effect is mainly used to increase the density of the sample, accelerating the diffusion of species to enlarge the bridges between particles. However, at higher densities, when the sample is close to be fully dense, grain growth can occur like in bulk samples. Considering the effect of time at a fixed temperature, as the sample exhibits already a high density at the temperature considered, the grain growth occurs. Anyway the effect of time is lower than that of temperature, which is well known in homogenization heat treatment of steels.

#### **IV. Conclusion:**

In this work, the molybdenum powder was sintered by SPS. Pressure and heating rate were fixed at 77 MPa and 700°C/min respectively. The sintering temperature was varied from 1200 to 1950°C and the holding time was varied from 5 to 30 minutes. The results of this investigation demonstrate that molybdenum powders can be successfully consolidated by SPS in very short times. The contact of the Mo powders with the graphite die and the carbon foil leads to the diffusion of carbon inside the samples to form a molybdenum carbide layer. The thickness of this layer depends on temperature and time and can reach 211  $\mu\text{m}$  at 1950°C. The carbide layer grows in a linear manner, with an activation energy of carbon diffusion in Mo equal to 34 Kcal/mol.

A relative density of 100% was achieved at a sintering temperature of 1850°C and a holding time of 30 minute. It can be concluded that the relative density is controlled by

temperature and time. Hardness measurements were made at different locations on the surface of each samples. It was shown that the hardness of Mo bulk decrease very slightly with temperature and time. The grain growth during SPS was controlled by the sintering temperature and time. The sintering temperature has a significant effect on grain size. When the sintering temperature is under 1450°C, the grain grow is slow and limited, while sintering temperature exceeding 1450°C result in the grain growing significantly. Moreover, it was also shown that the grain size increases with time.

## Acknowledgement

The authors would are pleased to acknowledge important contributions used in the body of this work from G. Bonnefont and F. Mercier from MATEIS for SPS processing, as well as to thank M. Perez from MATEIS for fruitful discussions.

## References

- [1] E.R Braithwaite, J. Haber: *Studies In Organic Chemistry*, 1994, vol. 19, pp. 662
- [2] J.A. Shields, E.L. Baker: *Adv. Mater. Process*, 1999, vol. 155, pp. 61-64.
- [3] E.F. Baroch, M. Ostermann, G. Patrick: *Adv. Powder Metall.*, 1991, vol. 5, pp. 321-331
- [4] T.S. Srivatsan, B.G. Ravi, M. Petraroli, T.S. Sudarshan: *Int. J. Refract. Met. Hard Mater.*, 2002, vol. 20, pp. 181-6
- [5] P. Garg, S.J. Park, R.M. German: *Int. J. Refract. Met. Hard Mater*, 2007, vol. 25, pp. 16-24
- [6] H. Schwarzbauer, R. Kuhnert: *IEEE Trans Ind Appl*, 1991, vol. 27, pp. 93-95
- [7] German RM, Labombard CA: *Int. J. Powder Metall. Powder Technol*, 1982, vol. 18, pp. 147-150
- [8] P.E. Zovas, R.M. German: *Metall. Trans*, 1983, vol. 15A, pp. 1103
- [9] H. Hofmann, M. Grosskopf, M. Hofmann-Anten-Brink, G. Petzow: *Powder Metall.*, 1986, vol. 29, pp. 201-6
- [10] Y. Hiraoka, T. Ogusu, N. Yoshizawa: *J. Alloys Compd.*, 2004, vol. 381, pp. 192-196
- [11] K.S. Hwang, H.S. Huang: *Acta Mater.* 2003, vol. 51, pp. 3915-26

- [12] K.S. Hwang, H.S. Huang: *Int. J. Refract. Hard Mater.*, 2004, vol. 22, pp. 185-91
- [13] R.M. German, Z.A. Munir: *J. Less-Common Met.*, 1978, vol. 58, pp. 61-74
- [14] L.E. Murr, M.A. Meyers, L.E. Murr: *Shock Waves and High Strain-Rate Phenomena: Concepts and Applications*, Plenum, New York, NY, 1981
- [15] M. Meyers, B.B. Gupta, L.E. Murr: *J. Met.*, 1981, vol. 33, pp. 21-26
- [16] D. Raybould, D. Morris, G. Cooper: *J. Mater. Sci.*, 1979, vol. 14, pp. 2523-26
- [17] A.M. Staver, M.A. Meyers, L.E. Murr: *Proc. Int. Cogherence Shock Waves High Strain Rate Phenom. Met.*, Plenum, New York, 1981, pp. 865
- [18] P. Kasiraj, P.J. Kasiraj, R.B. Schwarz, T.J. Ahrens: *J Materials Science*, 1984, vol. 32, pp.1235
- [19] R.V. Raman: *Adv. Mater. Process*, 1990, vol. 137, pp. 109
- [20] C.A. Kelto, E.E. Timm, A.J. Pyzik: *Annu. Rev. Mater. Sci.*, 1989, vol. 19, pp. 527-50
- [21] G. Jones, J.R. Groza, K. Yamazaki, K. Shoda: *Mater. Manuf. Process*, 1994, vol. 9, pp. 1105-14
- [22] J. Groza, S.H. Risbud, K. Yamazaki: *J Mater. Res.* 1992, vol. 7, pp. 2643
- [23] B.G. Ravi, P.D. Ramesh, N. Gupta, K.J. Rao: *J. Mater. Chem.*, 1997, vol. 7, pp. 2043-48
- [24] B.G. Ravi, V. Praveen, M.P. Selvam, K.J. Rao: *Mater. Res. Bull.*, 1998, vol. 33, pp. 1527-36
- [25] S.H. Yoo, T.S. Sudarshan, K. Sethuram, G. Subhash, R.J. Dowding: *Powder Metall*, 1999, vol. 42, pp. 181-82
- [26] T.S. Srivatsan, B.G. Ravi, A.S. Naruka, L. Riester, M. Petraroli, T.S. Sudarshan: *J. Powder Technol.*, 2001, vol. 114, pp. 136–144
- [27] Z. Shen, M. Nygren: *J. Mater. Chem.*, 2001, vol. 11, pp. 204-207
- [28] L. Gao, J.S. Hong, H. Miyamoto, S.D.D.L. Torre: *J. Eur. Ceram. Soc.*, 2000, vol. 20, pp. 2149-52
- [29] Z. Munir, U. Anselmi-Tamburini, M. Ohyanagi: *J. Mater Sci.*, 2006, vol. 41, pp. 763-77
- [30] D.M. Hulbert, A. Anders, J. Andersson, E.J. Lavernia, A.K. Mukherjee: *Scripta Mater.*, 2009, vol. 60, pp. 835-38
- [31] R. Ohser-Wiedemann, U. Martin, H.J. Seifert, A. Müller: *Int J Refract. Met Hard Mater*, 2010, vol. 28, pp. 550-57
- [32] E. Parthé, V. Sadogopan: *Acta Crystallogr.*, 1963, vol. 16, pp. 202-05
- [33] P. Liu, J.A. Rodriguez: *J. Chem. Phys.*, 2004, vol. 120, pp. 5414
- [34] K. Oshikawa, M. Nagai, S. Omi: *J Phys Chem B*, 2001, vol. 105, pp. 9124–31

- [35] L. Börnestein: *condens. Matter*, 2006, vol. 26
- [36] Y. Isobe, P. Son, M. Miyake: *J less-Common Metals*, 1989, vol. 147, pp. 261-68
- [37] S.M. Tuominen, J.M. Dahl: 108th AIME Annual Meeting, New Orleans, LA, Feb 1979
- [38] G.-S. Kim, H.G. Kim, D.-G. Kim, S.-T. Oh, M.-J. Suk, Y.D. Kim: *J. Alloys Compd.*, 2009, vol. 469, pp. 401-05
- [39] T.S. Srivatsan, B.G. Ravi, M. Petraroli, T.S. Sudarshan: *Int. J. Refract. Met. Hard Mater*, 2002, vol. 20, pp. 181-86

## Table Captions:

**Table 1:** Sintering parameters and results of density, hardness measurements and grain size

## Figures Captions

**Figure 1:** SEM micrograph of commercial Mo Powder before consolidation and after wet chemical etching. The average grain size is about 16  $\mu\text{m}$ .

**Figure 2:** Schematic drawing of Spark Plasma Sintering apparatus.

**Figure 3:** Cross sectional view of molybdenum sintered by SPS at 1850°C for 5 min, and with a pressure of 77 MPa (a) optical microscope and (b) Scanning Electron Micrograph. M1 and M2 represent the two different microstructures obtained in the same sample.

**Figure 4:** SIMS spectra collected on the superficial layer (M1) of the sample presented in figure 3.

**Figure 5:** XRD pattern of the molybdenum of the sample present in figure 3.

**Figure 6:** The square of layer thickness of the  $\text{Mo}_2\text{C}$  as a function of time. The dotted line is plotted to guide the eye. The growth rate is then parabolic in time.

**Figure 7:** Evolution of the  $\text{Mo}_2\text{C}$  layer growth rate as a function of the temperature. From the Arrhenius plot the apparent activation energy ( $E_A$ ) was estimated to be at 34 Kcal/mol.

**Figure 8:** Evolution of relative density and hardness a) as function of sintering temperature for a given time at 5 min and b) as function of holding time for a given temperature at 1850 °C.

**Figure 9:** a) Cross-sectional optical micrograph of bulk molybdenum after wet chemical etching at 1850°C for 5 min, and with a pressure of 77 MPa, b) grain size distribution, c) effect of sintering temperature on average grain size at a given time (5min) and c) effect of holding time on average grain size at 1850°C.

Sample	Sintering temperature (°C)	Holding Time (min)	Carbide Layer Thickness (µm)	Relative density with carbide layer (%)	Relative density without carbide layer (%)	Mo Hardness (Hv5)	Grain size (µm)
1	1200	5	-	84.4	84.4	133	16
2	1350	5	-	91.2	91.2	132	16
3	1450	5	-	94.8	94.8	160	33
4	1550	5	39	96.1	96.5	157	36
5	1650	5	56	96.1	97.0	161	42
6	1750	5	79	97.7	98.4	150	63
7	1850	5	132	97.7	98.6	150	82
8	1950	5	211	96.9	99.5	149	108
9	1850	10	187	97.3	99.6	157	83
10	1850	20	362	95.7	99.8	156	92
11	1850	30	391	94.5	100	156	102

**Table 1:** Sintering parameters and results of density, hardness measurements and grain size

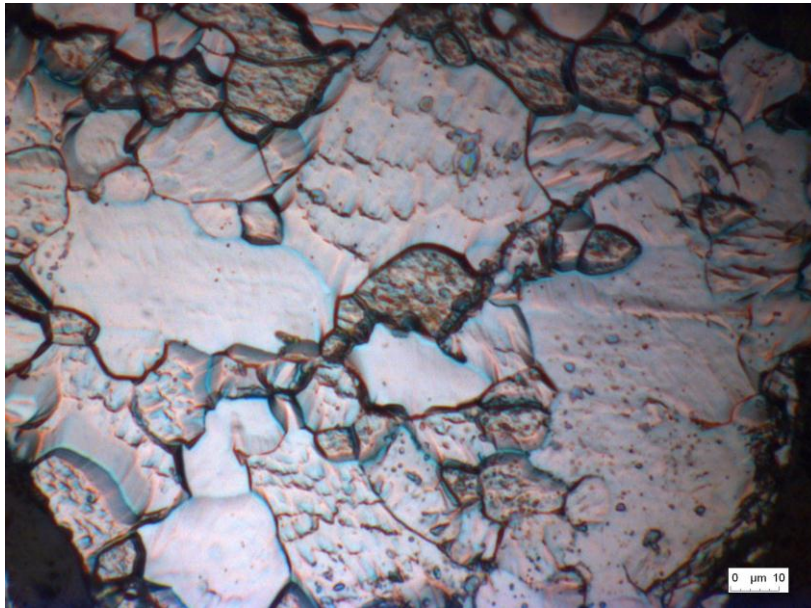


**Figure 1:** SEM micrograph of commercial Mo Powder before consolidation and after wet chemical etching. The average grain size is about 16  $\mu\text{m}$ .

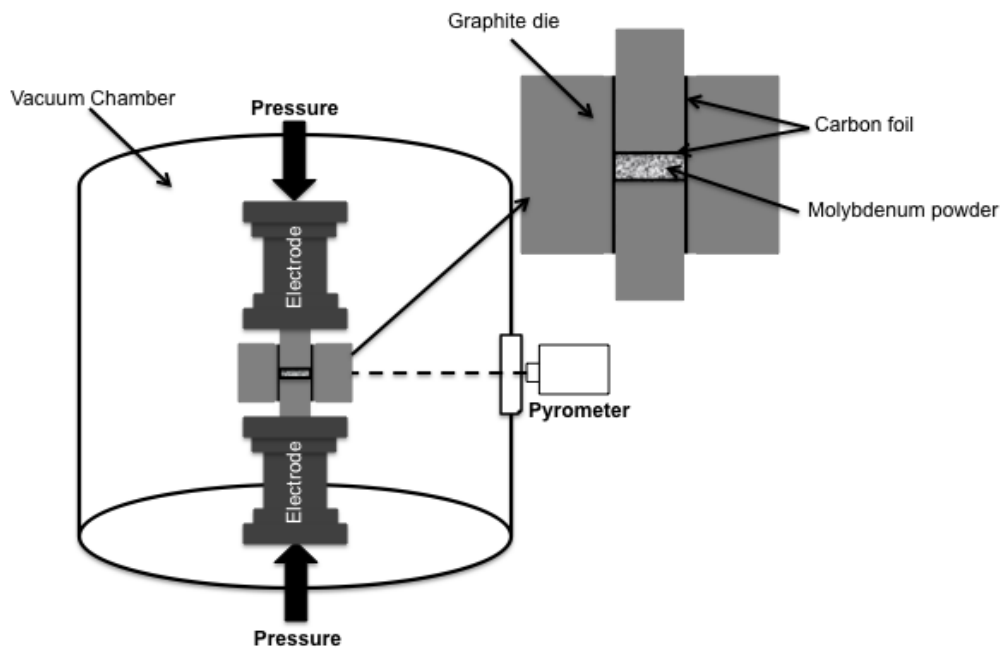


**Figure 2:** Schematic drawing of Spark Plasma Sintering apparatus.

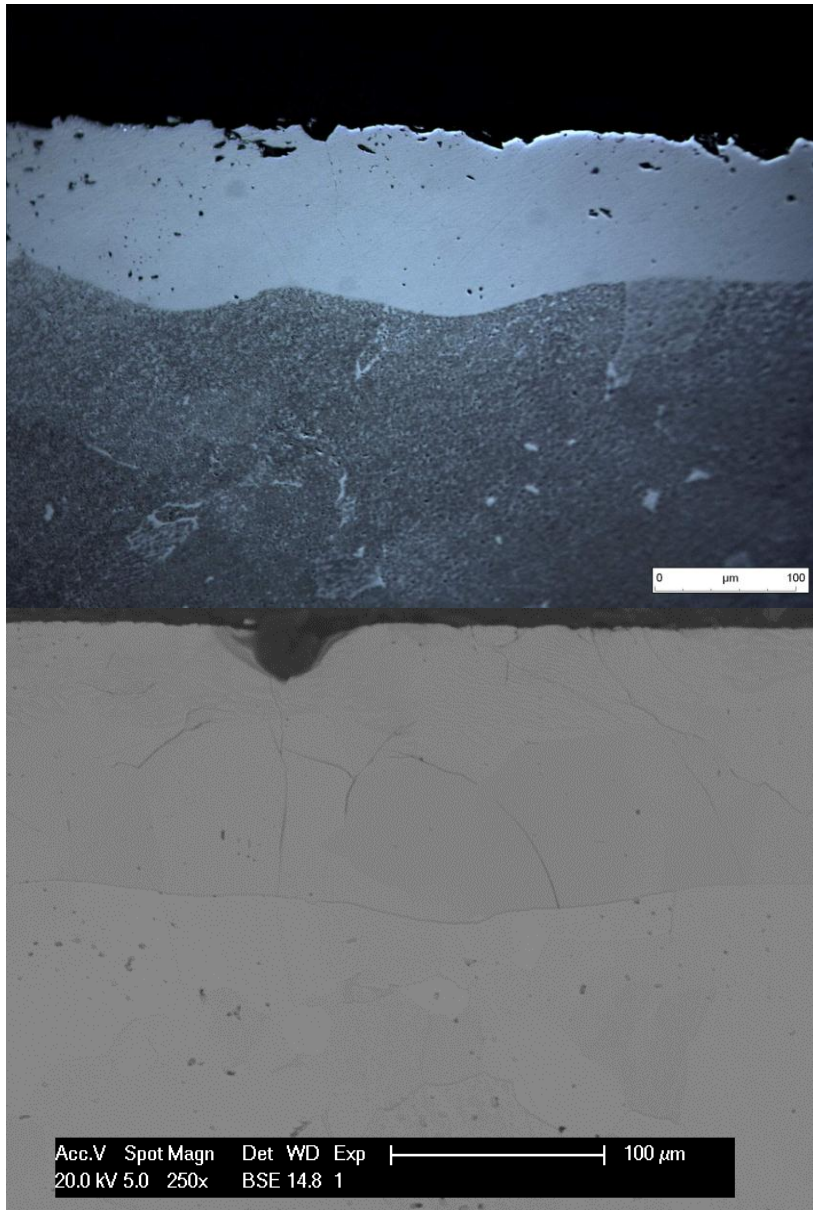


**Figure 3:** Cross sectional view of molybdenum sintered by SPS at 1850°C for 5 min, and with a pressure of 77 MPa (a) optical microscope and (b) Scanning Electron Micrograph. M1 and M2 represent the two different microstructures obtained in the same sample.

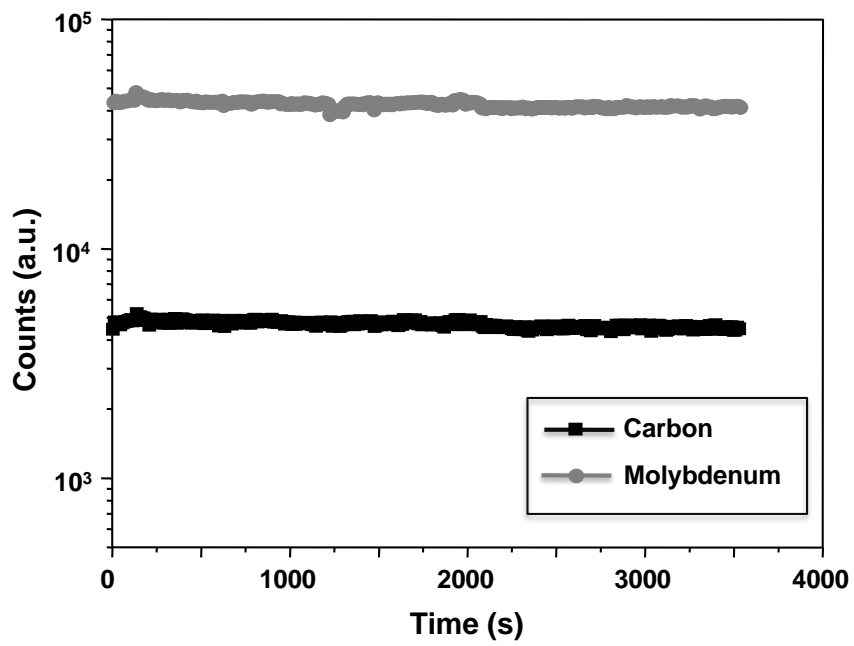


**Figure 4:** SIMS spectra collected on the superficial layer (M1) of the sample presented in fig.3.

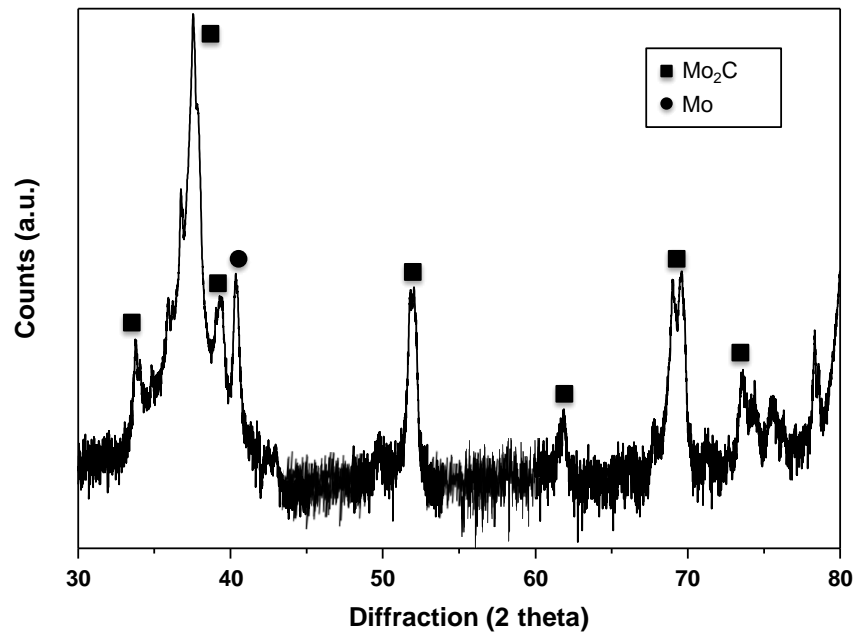


**Figure 5:** XRD pattern of the molybdenum of the sample present in figure 3.

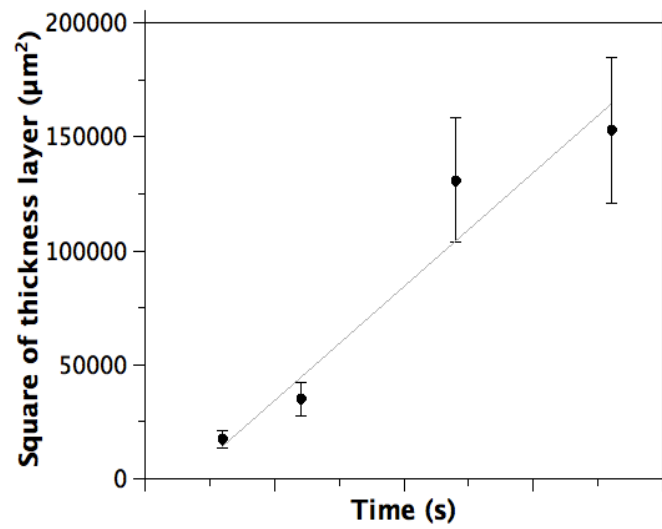


**Figure 6:** The square of layer thickness of the Mo<sub>2</sub>C as a function of time. The dotted line is plotted to guide the eye. The growth rate is then parabolic in time.

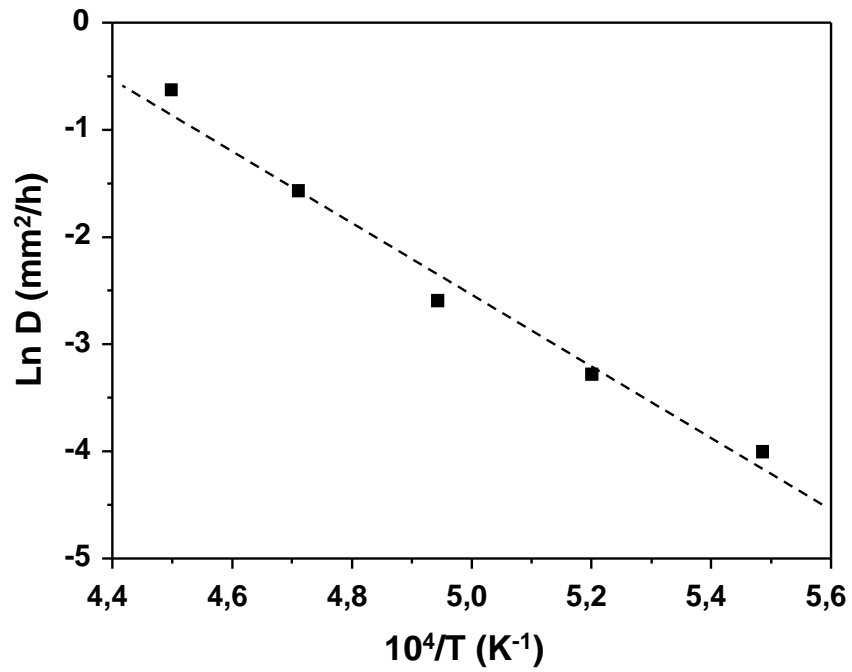


**Figure 7:** Evolution of the Mo<sub>2</sub>C layer growth rate as a function of the temperature. From the Arrhenius plot the apparent activation energy ( $E_A$ ) was estimated to be at 34 Kcal/mol.

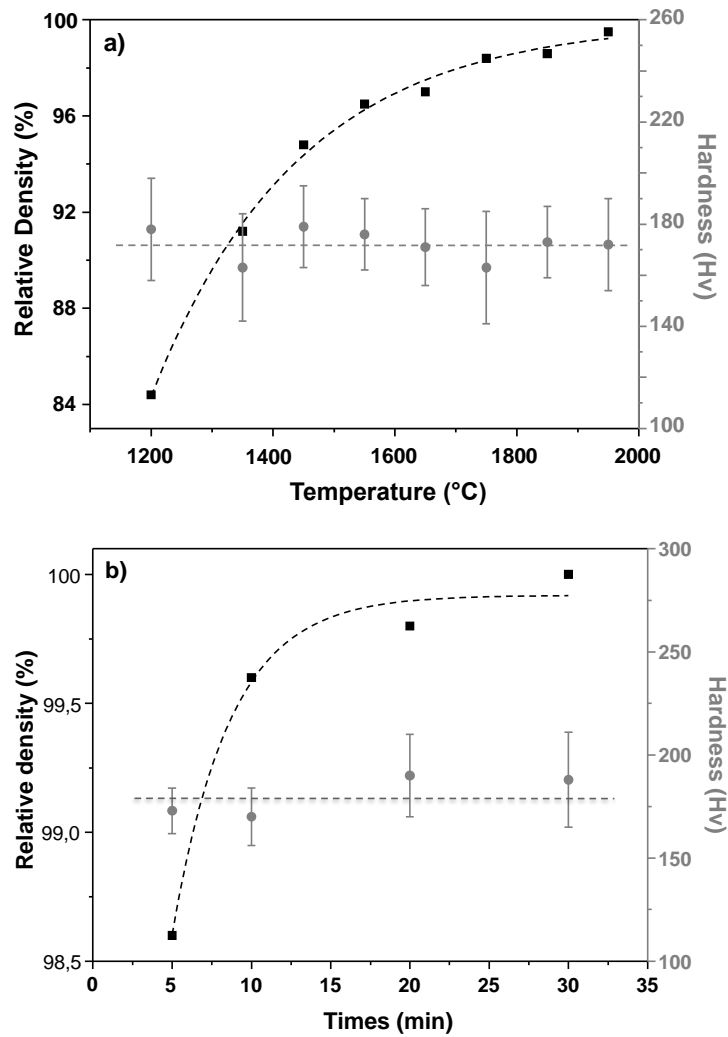


**Figure 8:** Evolution of relative density and hardness a) as function of sintering temperature for a given time at 5 min and b) as function of holding time for a given temperature at 1850 °C.

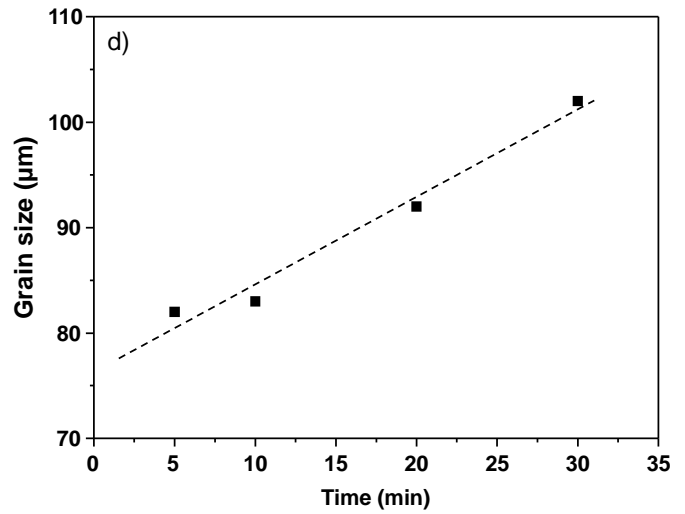
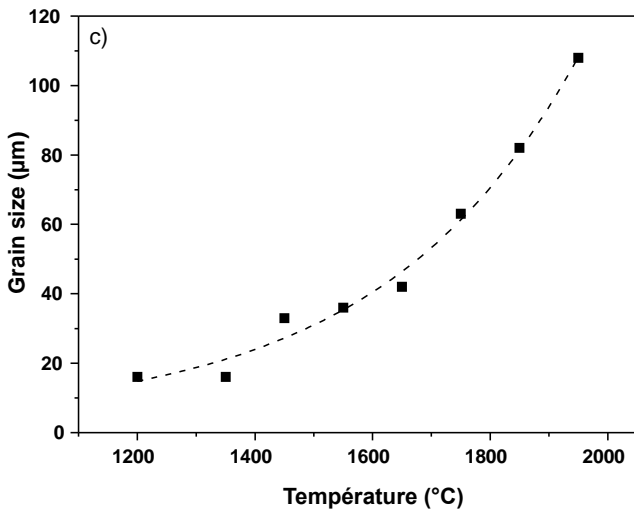
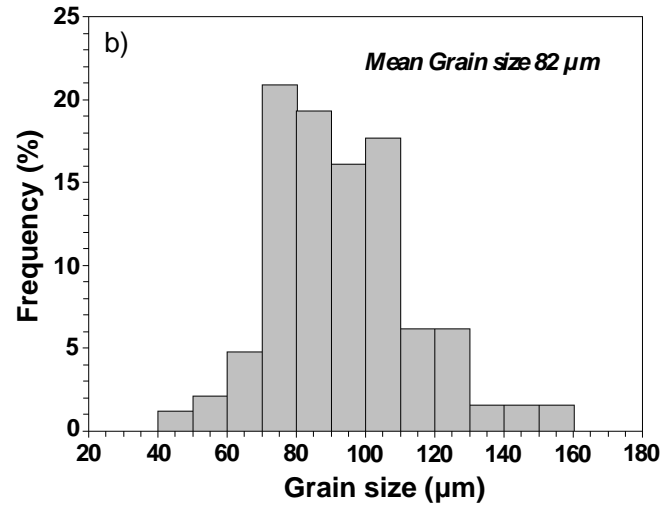
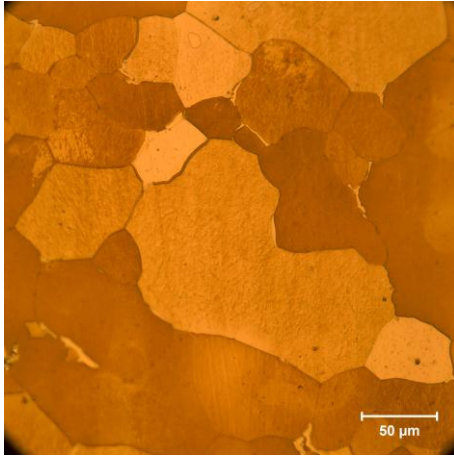


**Figure 9:** a) Cross-sectional optical micrograph of bulk molybdenum after wet chemical etching at 1850°C for 5 min, and with a pressure of 77 MPa, b) grain size distribution, c) effect of sintering temperature on average grain size at a given time (5min) and c) effect of holding time on average grain size at 1850°C.